JME

Journal of Mining & Environment,
Vol.8, No.4, 2017, 555-565.
DOI: 10.22044/jme.2016.781

Sub-pixel classification of hydrothermal alteration zones using a kernel-based method and hyperspectral data; A case study of Sarcheshmeh Porphyry Copper Mine and surrounding area, Kerman, Iran

A. Salimi[1]*, M. Ziaii[1], A. Amiri[2] and M. Hosseinjani Zadeh[3]

1. School of Mining, Petroleum & Geophysics Engineering, Shahrood University of Technology, Shahrood, Iran
2. Computer Engineering Group, Faculty of Engineering, University of Zanjan, Zanjan, Iran
3. Department of Ecology, Institute of Science and High Technology and Environmental Science, Graduate University of Advanced Technology, Kerman, Iran

Received 19 June 2016; received in revised form 20 September 2016; accepted 12 November 2016
**Corresponding author: a.salimi@shahroodut.ac.ir (A. Salimi)*

Abstract
Remote sensing image analysis can be carried out at the per-pixel (hard) and sub-pixel (soft) scales. The former refers to the purity of image pixels, while the latter refers to the mixed spectra resulting from all objects composing of the image pixels. The spectral unmixing methods have been developed to decompose mixed spectra. Data-driven unmixing algorithms utilize the reference data called training samples and end-members. The performance of algorithms using training samples can be negatively affected by the curse of dimensionality. This problem is usually observed in the hyperspectral image classification, especially when a low number of training samples, compared to the large number of spectral bands of hyperspectral data, are available. An unmixing method that is not highly impressed by the curse of dimensionality is a promising option. Among all the methods used, Support Vector Machine (SVM) is a more robust algorithm used to overcome this problem. In this work, our aim is to evaluate the capability of a regression mode of SVM, namely Support Vector Regression (SVR), for the sub-pixel classification of alteration zones. As a case study, the Hyperion data for the Sarcheshmeh, Darrehzar, and Sereidun districts is used. The main classification steps rely on 20 field samples taken from the Darrehzar area divided into 12 and 8 samples for training and validation, respectively. The accuracy of the sub-pixel maps obtained demonstrate that SVR can be successfully applied in the curse of dimensional conditions, where the size of the training samples (12) is very low compared to the number of spectral bands (165).

Keywords: *Hydrothermal Alteration, Hyperspectral Remote Sensing, Soft Classification, Spectral Unmixing, Support Vector Regression (SVR).*

1. Introduction

Hyperspectral remote sensing sensors provide high spectral resolution data compared to the conventional multi-spectral sensors. Using hundreds of contiguous spectral channels to measure reflected electromagnetic energy enables the hyperspectral sensors to produce huge and detailed spectral information about the earth surface materials. Analyzing this huge amount of data makes possible the uncovering of similar objects and materials of the earth surface [1-4].

Hyperspectral data is utilized by various types of applied sciences. The natural sciences and geosciences also use the hyperspectral data in geology, soil sciences, hydrology, etc. [5]. During the past two decades, the enhanced results of the hyperspectral-based mineral mapping have made it an important tool to study various types of surface minerals and rocks [6-7]. The field of mineral deposit exploration also enjoys this unique ability of the hyperspectral technology by identification of the indicator minerals and rocks

corresponding to the mineral deposits. Essentially, the lithological anomaly detection is known as a mineral exploration method besides the geochemical and geophysical approaches. Hydrothermal alteration rocks are a kind of lithological anomalies that have resulted from a chemical interaction between the host rocks and the hydrothermal fluids. Spatially, the alteration rocks are related to the outflow zones of the hydrothermal systems, and can be applied to locate mineral deposits [8]. The hydrothermal alteration mineral mapping through hyperspectral remote sensing has been widely and successfully performed for the exploration of various hydrothermal deposits [9].

The hard and soft classifications are two familiar concepts in remote sensing image analysis. In the hard case, it is supposed that each pixel is completely pure and contains merely one kind of material. The soft type refers to mixed pixels with this assumption that more than one material contribute to the pixels of image [10]. Clearly speaking, the hard and soft classifications refer to the per-pixel and sub-pixel analysis, respectively. It is so much probable that a lot of mixed pixels exist in remote sensing images, especially in low spatial resolution images with relatively large pixels [10-12]. At these scales, every pixel can be included by several types of materials or objects, and therefore, the measured spectrum of a pixel is a combination of spectra resulting from all objects within the pixel. In addition to the size of pixels, spectral mixing can happen at small scales like mineralogy, in which a small rock sample is a mixture of several minerals [10].

The hard classification of images containing many mixed pixels can lead to many errors and no reliable results [13]. In the recent years, a lot of algorithms have been developed to decompose mixed pixels into their class components and to estimate the abundance of each component, which have been called the spectral unmixing methods in the literature [4, 10, 14-15]. The unmixing methods in the taxonomical tree of spectral processing methods are categorized as data-driven approaches (Figure 1) [16]. The data-driven methods apply reference data that is based on the utilized algorithm called training samples or end-members. Training samples are a set of labeled data containing several features that are applied to train algorithms. These features in the remote sensing field are the spectral bands of images [16].

The size of the training samples with respect to the features has an important role in the performance of algorithms so that the insufficient training samples with respect to the feature space size can be led to curse of dimensionality and an important ill-posed problem, i.e. the Hughes phenomenon [17-19]. These problems can be potentially observed in the classification of hyperspectral images because they contain a high number of spectral bands as the features. Therefore, preparing enough training samples with respect to the number of spectral bands cannot be an easy work, especially when it is tried to gather the training samples from the studied area. To take into account this specific nature of the hyperspectral images, the competent techniques are required because the traditional approaches cannot successfully analyze the massive size of hyperspectral data [19]. Among the data-driven unmixing methods (Figure 1), the kernel-based SVM method is a more promising algorithm to handle the curse of dimensionality and Hughes phenomenon, especially when the size of the training dataset is limited [2-3, 18, 20-22].

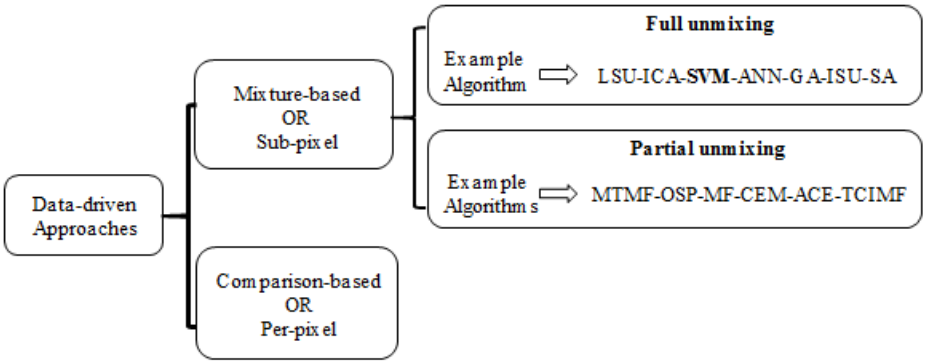

Figure 1. A part of taxonomic tree of spectral processing methods covering unmixing algorithms. Acronyms are as what follow. LSU: linear spectral unmixing, ICA: independent component analysis, SVM: support vector machine, ANN: artificial neural network, GA: genetic algorithm, ISU: iterative spectral unmixing, SA: simulated annealing, MTMF: mixture-tuned matched filtering, OSP: orthogonal sub-space projection, MF: matched filtering, CEM: constrained energy minimization, ACE: adaptive coherence estimator (Modified from Ref. [16]).

The widespread hard and soft applications of SVM in the extensive applied fields have been presented as a detailed review study by Ref. [21]. Also in the review study of Ref. [10] about non-linear hyperspectral unmixing, a section has been devoted to unmixing and soft classification by SVM.

In this paper, SVR as the regression mode of SVM is used for soft classification. SVM is utilized at the simplest mode to predict discrete targets, while SVR not only utilizes the same theoretical concepts of SVM but also predicts continuous variables. Therefore, SVR can be employed to predict the abundance of the components of pixels and to generate fractional classified images [23]. SVR has not previously been widely used to map minerals and alteration zones.

Therefore, the main objective of this study is the soft classification of the alteration zones using a hyperspectral data and SVR, a consistent data-driven method for the hyperspectral data analysis. Preparing sufficient ground truth rock samples as the training samples requires a field survey, which is usually time-consuming and costly. Therefore, we want to evaluate the performance of SVR when it is applied to classify the Hyperion hyperspectral data by few numbers of training samples. Increasing the curse of dimensionality is the main aim of using a limited size training set (12 samples in this study) compared to the great number of Hyperion spectral bands (165 useable bands).

Our studied area was the Sarcheshmeh and Darrehzar porphyry type copper mines and Sereidun district. Due to the importance of the studied area, its alteration zones have been studied by various researchers and many kinds of methods and remote sensing data. In some of the studies, the multi-spectral data [24-27] has been utilized, and some others have employed the hyperspectral data [28-29]. From the viewpoint of applied methods, there are comparison-based methods for hard classification such as spectral angle mapper (SAM) [24, 26] and mixture-based methods for soft classification such as Mixed Tuned Match Filtering (MTMF) [25, 28] and Linear Spectral Unmixing (LSU) [24].

2. Geological setting of studied area

The studied area was Sarcheshmeh Copper Mine and the eastern, southern, and SE area of Sarcheshmeh including the Darrehzar mine and Sereidun district. These areas are located in the southern part of the Uromiyeh-Dokhtar Cenozoic magmatic belt (Figure 2a). This belt with a length of 1800 Km encloses many types of copper, molybdenum, and gold mineralization such as the important mines like Sarcheshmeh, Sungon, and Meydouk [30].

The giant Sarcheshmeh deposit with the 1200 Mt ore and the average grade of 0.69% Cu and 0.03% Mo is known as a typical porphyry Cu deposit [30]. The alteration types of Sarcheshmeh from the center to outward are potassic, biotitic, phyllic, argillic, and propylitic, which are the same with the alterations of typical porphyry Cu deposits [30-31]. Potassic is affected by phyllic, strongly phyllic, and propylitic alterations form spatial arrangement of its alterations from center to outside of the deposit [32]. The Darrehzar porphyry copper deposit is located 8 km to the SE of Sarcheshmeh. It has almost 67 Mt of the estimated ore mineral reserve with the average grade of 0.37% Cu [33]. Eocene volcano-sedimentary rocks have hosted mineralized diorite and granodiorite formations. Hydrothermal fluids have extensively altered these formations into potassic, phyllic, propylitic, and argillic products. The dimensions of the alteration zones at the length and width are about 2.2 km and 0.7–1 km, respectively. The phyllic and argillic zones are surrounded by the propylitic zone. Although the mentioned zones are extensively seen in most parts of the area; because of the surface related to weathering, there is no potassic alteration at the surface [34]. The Sereidun district, situated in the east vicinity of Sarcheshmeh, is composed of different types of hydrothermal alterations such as propylitic, phyllic, argillic, and advanced argillic (Figure 2b) [35].

3. Materials and method

3.1. Hyperion dataset

The data for the hyperspectral Hyperion sensor, acquired on 26 July 2004, was utilized in this research work. Our studied area in the available scene of Hyperion can be seen in Figure 3. The image spectrum of the three indicator minerals corresponding to different alteration zones with their diagnostic spectral absorptions are shown in Figure 4. After a pre-processing step, 77 spectral bands for all the 242 available Hyperion bands were removed, and subsequently, the remaining 165 bands were used for further processing (Table 1). A detailed explanation of the pre-processing step is comprehensively explained in Ref. [36].

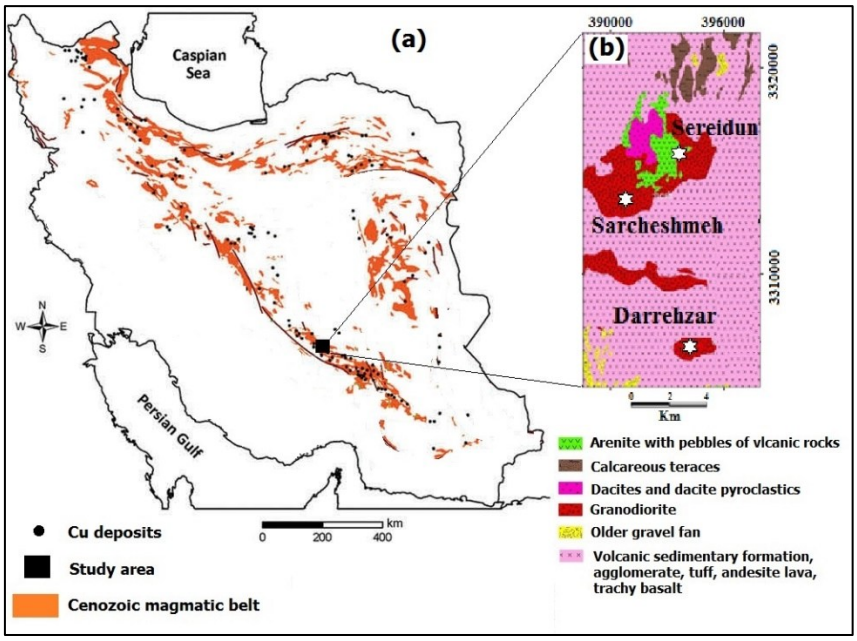

Figure 2. (a) Location of Cenozoic magmatic belt and studied area in Iran (Modified from Ref. [26]), (b) Geological map of studied area and locations of three copper deposits: Sarcheshmeh, Sereidun, and Darrehzar (Modified from Ref. [28]).

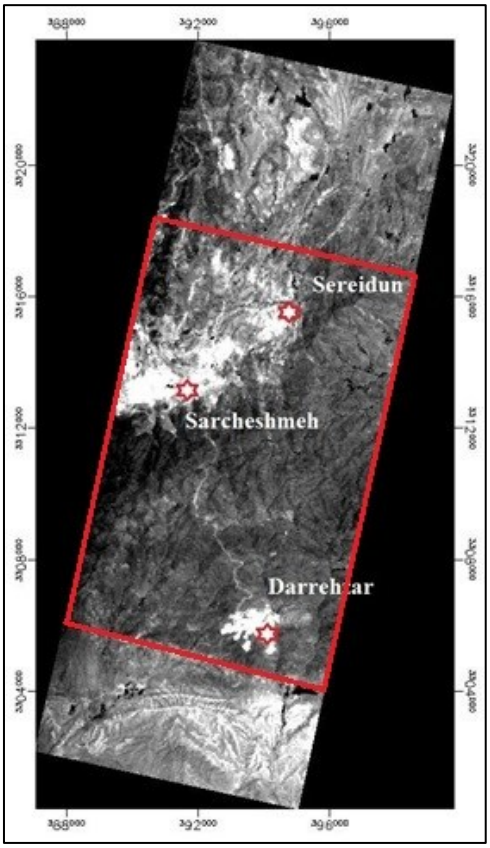

Figure 3. Studied area in Hyperion scene, and locations of Sarcheshmeh, Sereidun, and Darrehzar.

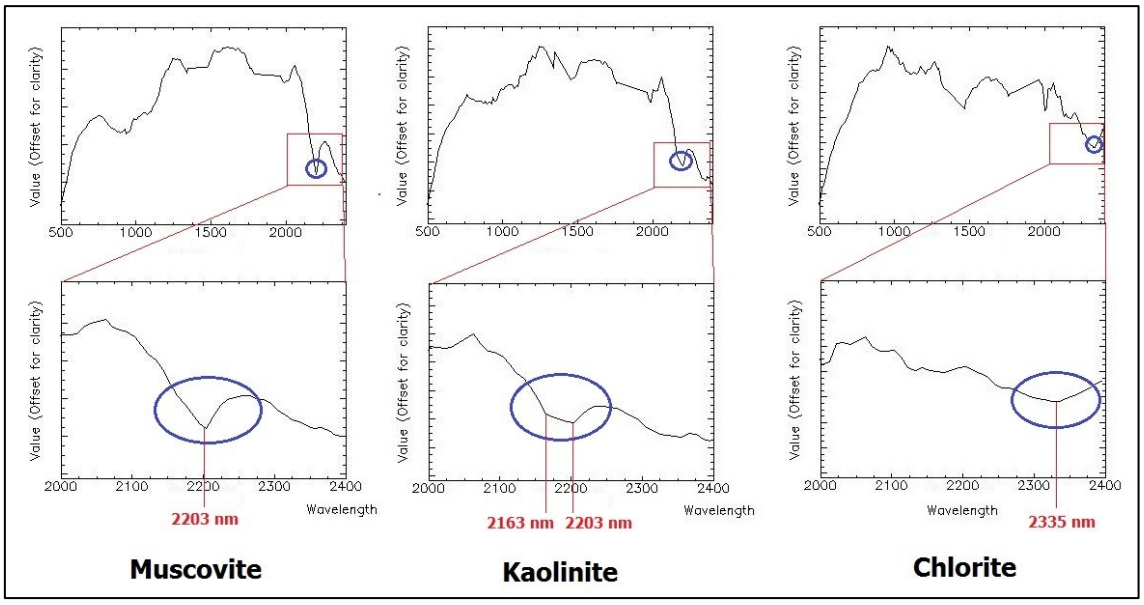

Figure 4. Hyperion image spectra of muscovite, kaolinite, and chlorite corresponding to phyllic (Darrehzar), argillic (Sereidun), and propylitic (Darrehzar) zones, respectively. Diagnostic spectral absorption of each mineral is also illustrated in each case.

Table 1. 165 bands of Hyperion after pre-processing.

Bands	Wavelength (nm)
8–57	426–925
79–93	932–1073
95–98	1094–1124
100-115	1144–1295
117–120	1316–1346
131–164	1457–1790
181–189	1961–2042
191–202	2062–2173
204–224	2193–2395

3.2. Training, testing, and validation dataset (ground truth samples)

Supervised unmixing methods require a training sample set to properly learn the discriminative rules of patterns. Moreover, another sample set is usually required to validate the performance and generalization capacity of classification. In this research work, these datasets were selected from 20 samples gathered from the Darrehzar area. To evaluate the robustness of the SVR regarding a small size training set, it was tried to apply a small number of field samples. Therefore, 12 rock samples of alteration zones were selected as the training samples, and the 8 remaining samples were used as the validation samples. All samples were spectrally measured using analytical spectral devices (ASD) at the department of Ecology, Institute of Science and High Technology and Environmental Science, Graduate University of Advanced Technology, Kerman, Iran. The ASD output was analyzed by an automated mineral identification program, namely PIMA View, to see the semi-quantitative abundance of some alteration minerals. Abundances of the indicator minerals of the propylitic, phyllic, and argillic zones were applied to train SVR, and then the sub-pixel prediction was performed. The semi-quantitative abundances of chlorite, muscovite, and kaolinite are seen in the abundance column of Table 2. The spatial distribution of the field samples is shown in Figure 5.

Table 2. Semi-quantitative abundance of three indicator minerals of alteration zones in 12 field samples (training samples) obtained by PIMA View program.

No.	(type)	Abundance (PIMA View output) (%)		
	Alteration	Chlorite	Muscovite	Kaolinite
1	Phyllic	< 5	65	20
2	Phyllic	< 5	70	< 5
3	Phyllic	< 5	75	< 5
4	Phyllic	< 5	75	< 5
5	Argillic	< 5	20	45
6	Argillic	< 5	35	50
7	Argillic	< 5	30	65
8	Propylitic	30	< 5	< 5
9	Propylitic	40	35	< 5
10	Propylitic	45	30	< 5
11	Propylitic	60	< 5	< 5
12	Propylitic	35	15	< 5

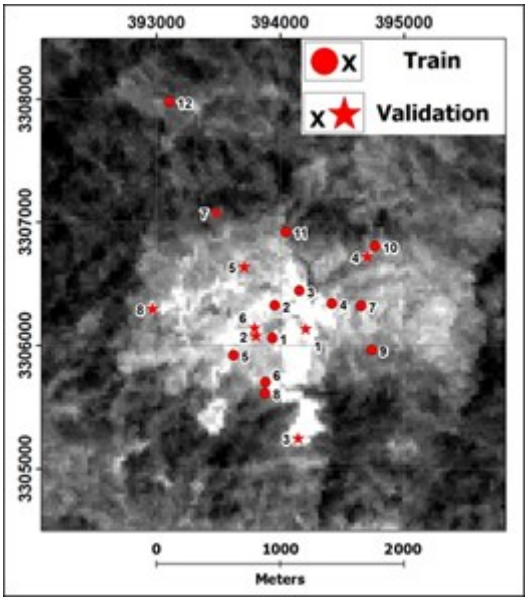

Figure 5. Location of 12 training samples (Table 2) and 8 validation samples (Table 4).

3.3. Support Vector Regression (SVR)

SVM and SVR have been investigated in detail in Ref. [37]. SVR utilizes the concepts of SVM for regression and function estimation. Similar to SVM, based on the structural risk minimization, an optimal hyperplane is defined on the basis of the available training samples [20, 23]. The defined hyperplane of SVM discriminates the data samples of the two classes, while the SVR hyperplane is used as a function to estimate a target variable. In the linear case, it estimates the linear dependency of the input training samples and the target variables. The non-linear estimation is also possible using the kernel trick functions. C is the parameter of SVR, which is exactly the same with the SVM parameters and plays the same role in both cases. In addition to C, SVR applies ε, which controls the width of the margin. SVR tries to minimize a cost function with maximizaton of the margin and minimization of the approximation error [23]. This goal is formulated as follow [20]:

$$\begin{cases} \min\left\{\frac{1}{2}\left\|\vec{W}\right\|^2 + C\sum_{i=1}^{n}(\xi_i + \xi_i^*)\right\} \\ y_i - \vec{W}.\vec{X}_i - b \le \varepsilon + \xi_i \qquad \forall i = 1,...,n \\ \vec{W}.\vec{X}_i + b - y_i \le \varepsilon + \xi_i^* \qquad \forall i = 1,...,n \\ \xi_i, \xi_i^* \ge 0 \qquad \forall i = 1,...,n \end{cases}$$

Where ξ_i and ξ_i^* are the slack variables and C is the penalization parameter. The above optimization problem can be solved using the Lagrange multipliers (α), computing the Karush-Kuhn-Tucker (KKT) conditions and solving the obtained dual problem by the quadratic programming [37].

4. Results and discussion

4.1. Soft classification by SVR

Using the Hyperion image of the studied area and 20 field samples, the soft classification of the alteration zones were performed by SVR. Figure 6 is a flowchart, briefly showing four steps of the classification process including: i. Adjustment of parameters of SVR, ii. Training of SVR, iii. Alteration mapping by the trained SVR, and iv. Validation.

Abundances of three indicator minerals of 12 field samples (Table 2) were utilized by SVR for the soft or sub-pixel classification of the alteration zones in the studied area. Due to the outperformed results compared to the other kernel functions, the Radial Basis Function (RBF) was used to implement the non-linear SVR [38, 39]. To set the optimum values for parameters of SVR (C and ε) and RBF (σ), the leave-one-out cross-validation technique, which is appropriate for the limited size datasets, was implemented as follows: ε (from 5 to 20 with the interval distance of 5), C (from 500 to 5000 with the interval distance of 500), and σ (from 0.1 to 1 with the interval distance of 0.05). As mentioned in section 3.3, ε is an extra parameter for SVR that controls the acceptable error of the estimated variable. The assignment of at least 5% and at most 20% for ε can be justifiable because the semi-quantitative measured values for the mineral abundance by PIMA View are in percent. In other words, the assignment of at most 20% for error tolerance of a semi-quantitative measurement can be a reasonable choice. The optimum values for these parameters and their corresponding root mean square error (RMSE) obtained by the leave-one-out cross-validation error estimator are displayed in Table 3.

The trained SVR by the optimum parameters (Table 3) was utilized to map the alteration zones in the studied area. The final sub-pixel classified maps of the three indicator minerals is illustrated in Figure 7.

4.2. Validation

The 8 field samples unseen by SVR were used for validation. These results are represented in Table 4. The abundances of minerals for each sample are also found in this table. These values were semi-quantitatively estimated using the PIMA View software.

It can be observed in Table 4 that the estimated abundance of some samples by SVR are negative values or sum of the abundance values is more than 100%, both of which are meaningless. We can address these to the erroneous training samples and the semi-quantitative nature of the PIMA View program as the main reasons for observing such meaningless values. The collected training field samples are very small compared to the pixels of Hyperion image covering an area equal to 30 × 30 m^2. Therefore, this sampling cannot be quite representative.

For a visual comparison, soft predictions of SVR are also illustrated in Figures 8a, 8b, and 8c with location of validation samples in the alteration map of the Darrehzar area.

Table 3. Optimum parameters for SVR using leave-one-out cross-validation.

Class		SVR Parameters			RMSE (%)
Alteration zone	Indicator mineral	ε	C	σ	Leave-One-Out cross-validation
Propylitic	Chlorite	15	5000	0.2	20.92
Phyllic	Muscovite	10	3000	0.15	27.25
Argillic	Kaolinite	5	5000	0.15	23.35

Table 4. Semi-quantitative abundance of three indicator minerals of alteration zones in 8 field samples (validation samples) obtained by PIMA View program. Estimated abundance of each sample by SVR has also been reported.

No.	SVR (%)			PIMA View (%)		
	Chlorite	Muscovite	Kaolinite	Chlorite	Muscovite	Kaolinite
1	04	58	27	10	55	< 5
2	-14	58	46	< 5	55	40
3	-06	77	25	< 5	70	25
4	20	32	08	< 5	60	20
5	28	48	10	< 5	70	25
6	-09	52	57	< 5	30	65
7	44	-02	07	35	< 5	< 5
8	35	33	11	40	20	< 5

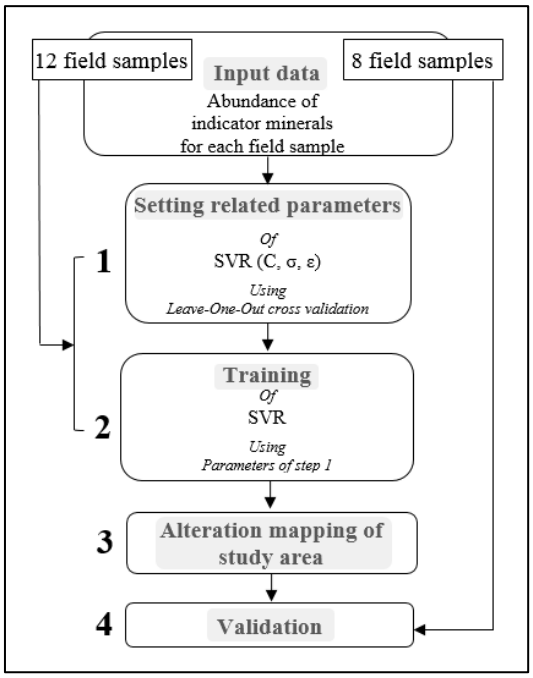

Figure 6. Flowchart of soft classification using SVR.

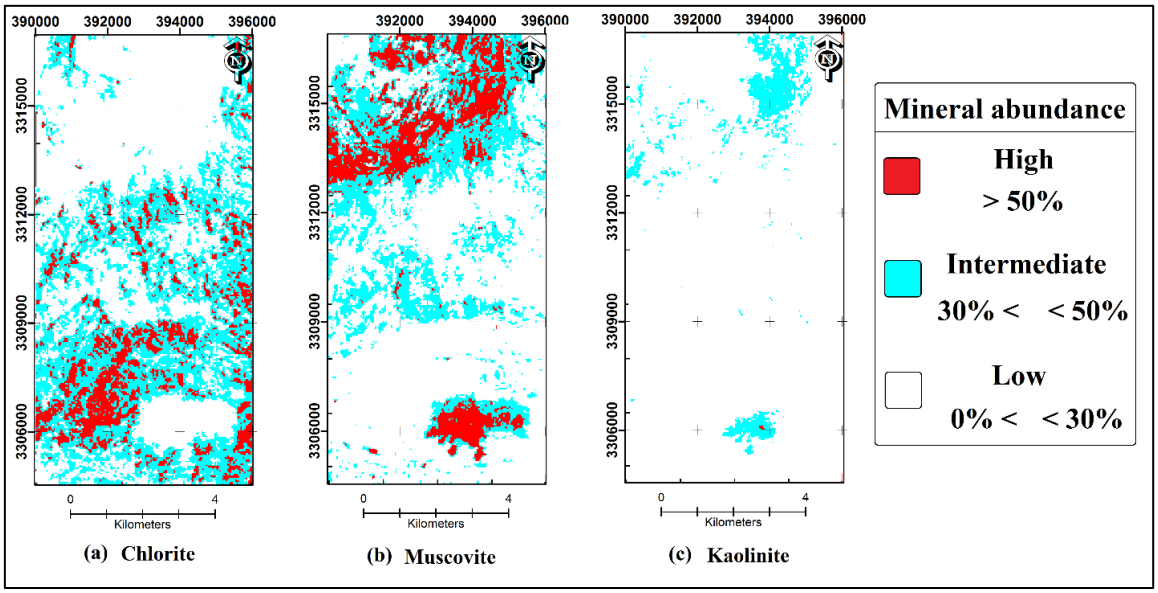

Figure 7. Sub-pixel or soft classified maps of alteration zones resulting from SVR: (a) Chlorite (propylitic), (b) Muscovite (phyllic), and (c) Kaolinite (argillic).

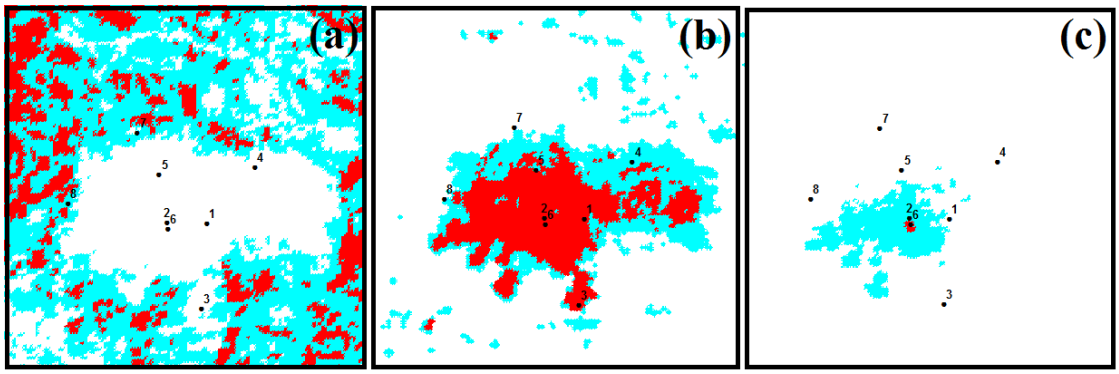

Figure 8. Locations of 8 validation field samples taken from studied area on soft alteration maps of SVR: (a) chlorite map (b) muscovite map (c) kaolinite map.

5. Conclusions

An appropriate method for hyperspectral data classification, namely SVR, was applied to the map alteration zones at the sub-pixel scale. The main advantage of SVR is its high ability in classifying high dimensional problems, especially where ground truth data is not properly available for training step. To evaluate this capability, the training phase was performed using a small number of samples (12 field samples). The adjustment of the SVR parameters is very important. Their incorrect estimation can strongly impress the accuracy of classification. To set the optimum values for these parameters, the leave-one-out cross-validation technique was utilized, which is a proper option for small datasets. Finally, the sub-pixel alteration maps were produced by SVR, and the results obtained were validated by 8 validation samples, which had no contribution to the classification phase. On the basis of the acceptable accuracies of the results, it was concluded that SVR could be successfully applied to the sub-pixel classification of alteration zones using high dimensional hyperspectral data.

Acknowledgments

The authors are grateful to the staff of the National Iranian Copper Industries Company, especially Sarcheshmeh and Darrehzar copper mines. We are sincerely thankful to Mr. Khosrojerdi and Mr. Salajegheh, who provided us with the facilities, kindly helping and expertise during our field work.

References

[1]. Bioucas-Dias, J.M., Plaza, A., Camps-Valls, G., Scheunders, P., Nasrabadi, N.M. and Chanussot, J. (2013). Hyperspectral Remote Sensing Data Analysis and Future Challenges. IEEE Geoscience and remote sensing magazine. 1 (2): 6-36. doi:10.1109/MGRS.2013.2244672.

[2]. Camps-Valls, G., Tuia, D., Bruzzone, L. and Benediktsson, J. (2014). Advances in Hyperspectral Image Classification. IEEE Signal Processing Magazine. 31 (1): 45-54. doi:10.1109/MSP.2013.2279179.

[3]. Chang, C. (2007). Hyperspectral Data Exploitation, Theory and Applications. Published by John Wiley & Sons, Inc. Hoboken. New Jersey. 430 P.

[4]. Keshava, N. and Mustard, J.F. (2002). Spectral unmixing. IEEE Signal Processing Magazine. 19 (1): 44-57. doi:10.1109/79.974727.

[5]. Van der Meer, F.D. and Van der Werff, H. (2007). Spatial-spectral contextual image analysis of hyperspectral data to aid in the characterization of hydrothermal alteration in epithermal gold deposits. In: New Developments and Challenges in Remote Sensing. pp. 275-285.

[6]. Wang, Z.H. and Zheng, C.Y. (2010). Rocks/Minerals Information Extraction from EO-1 Hyperion Data Base on SVM. International Conference on Intelligent Computation Technology and Automation. 3: 229-232. doi:10.1109/ICICTA.2010.341.

[7]. Zhang, X. and Peijun, L. (2014). Lithological mapping from hyperspectral data by improved use of spectral angle mapper. International Journal of Applied Earth Observation and Geoinformation. 31: 95-109. doi:10.1016/j.jag.2014.03.007.

[8]. Carranza, E.J.M. (2002). Geologically-Constrained Mineral Potential Mapping. Ph.D. Dissertation. Delft University of Technology. The Netherlands. 480 P.

[9]. Gersman, R., Ben-Dor, E., Beyth, M., Avigad, D., Abraha, M. and Kibreba, A. (2008). Mapping of hydrothermal altered rocks by the EO-1 Hyperion sensor, northern Danakil, Eritrea. International Journal of Remote Sensing. 29 (13): 3911-3936. doi:10.1080/01431160701874587.

[10]. Heylen, R., Parente, M. and Gader, P. (2014). A review of nonlinear hyperspectral unmixing methods. IEEE Journal of Selected Topics in Applied Earth Observations and Remote Sensing. 7 (6): 1844-1868. doi:10.1109/JSTARS.2014.2320576.

[11]. Villa, A., Chanussot, J., Benediktsson, J.A. and Jutten, C. (2011). Spectral Unmixing for the Classification of Hyperspectral Images at a Finer Spatial Resolution. IEEE Journal of Selected Topics in Signal Processing. 5 (3): 521-533. doi:10.1109/JSTSP.2010.2096798.

[12]. Wang, L. and Jia, X. (2009). Integration of Soft and Hard Classifications Using Extended Support Vector Machines. IEEE Geoscience and Remote Sensing Letters. 6 (3): 543-547. doi:10.1109/LGRS.2009.2020924.

[13]. Watanachaturaporn, P., Arora, M.K., Varshney, P.K. and Sveinsson, J.R. (2006). Sub-Pixel land cover classification using support vector machines. In: ASPRS 2006 Annual Conference. Reno. Nevada. 1-5 May.

[14]. Parente, M. and Plaza, A. (2010). Survey of geometric and statistical unmixing algorithms for hyperspectral images. In: Workshop on Hyperspectral Image and Signal Processing: Evolution in Remote Sensing (WHISPERS). Pp. 1-4. doi:10.1109/WHISPERS.2010.5594929.

[15]. Yanfeng, G.U., Wang, S. and Xiuping, J. (2013). Spectral Unmixing in Multiple-Kernel Hilbert Space for Hyperspectral Imagery. IEEE Transactions on Geoscience and Remote Sensing. 51 (7): 3968-3981. doi:10.1109/TGRS.2012.2227757.

[16]. Asadzadeh, S. and De Souza Filho, C.R. (2016). A review on spectral processing methods for geological remote sensing. International Journal of Applied Earth Observation and Geoinformation. 47: 69-90. doi:10.1016/j.jag.2015.12.004.

[17]. Alajlan, N., Bazi, Y., Melgani, F. and Yager, R. (2012). Fusion of supervised and unsupervised learning for improved classification of hyperspectral images. Journal of Information Sciences. 217: 39-55. doi:10.1016/j.ins.2012.06.031.

[18]. Pal, M. and Foody, G.M. (2010). Feature Selection for Classification of Hyperspectral Data by SVM. IEEE Transactions on Geoscience and Remote Sensing. 48 (5): 2297-2307. doi:10.1109/TGRS.2009.2039484.

[19]. Plaza, A., Benediktsson, J.A., Boardman, J.W., Brazile, J., Bruzzone, L., Camps-Valls, G., Chanussot, J., Fauvel, M., Gamba, P., Gualtieri, A., Marconcini, M., Tilton, J.C. and Trianni, G. (2009). Recent advances in techniques for hyperspectral image processing. Remote Sensing of Environment. 113: 110-122. doi:10.1016/j.rse.2007.07.028.

[20]. Gómez-Chova, L., Muñoz-Marí, J., Laparra, V., Malo-López, J. and Camps-Valls, G. (2011). A Review of Kernel Methods in Remote Sensing Data Analysis. In book: Optical Remote Sensing- Advances in Signal Processing and Exploitation Techniques, Publisher: Springer-Verlag, Editors: Saurabh, P. and Bruce, L. and Chanussot, J. pp.171-206. doi:10.1007/978-3-642-14212-3_10.

[21]. Mountrakis, G., Im, J. and Ogole, C. (2011). Support vector machines in remote sensing: A review. ISPRS Journal of Photogrammetry and Remote Sensing. 66: 247-259. doi: 10.1016/j.isprsjprs.2010.11.001.

[22]. Waske, B., Benediktsson, J.A., Arnason, K. and Sveinsson, J.R. (2009). Mapping of hyperspectral AVIRIS data using machine-learning algorithms. Canadian Journal of Remote Sensing. 35 (1): 106-116.

[23]. Okujeni, A., Van der Linden, S., Tits, L., Somers, B. and Hostert, P. (2013). Support vector regression and synthetically mixed training data for quantifying urban land cover. Remote Sensing of Environment. 137: 184-197. doi:10.1016/j.rse.2013.06.007.

[24]. Honarmand, M., Ranjbar, H. and Shahabpour, J. (2011). Application of spectral analysis in mapping hydrothermal alteration of the Northwestern Part of the Kerman Cenozoic Magmatic Arc, Iran. Journal of Sciences, Islamic Republic of Iran. 22 (3): 221-238.

[25]. Hosseinjani Zadeh, M., Tangestani, M.H., Velasco Roldan, F. and Yusta, I. (2014). Mineral exploration and alteration zone mapping using mixture tuned matched filtering approach on ASTER data at the central part of Dehaj-Sarduiyeh copper belt, SE Iran. IEEE selected topics in applied earth observations and remote sensing. 7 (1): 284-289. doi:10.1109/JSTARS.2013.2261800.

[26]. Shahriari, H., Honarmand, M. and Ranjbar, H. (2015). Comparison of multi-temporal ASTER images for hydrothermal alteration mapping using a fractal-aided SAM method. International Journal of Remote Sensing. 36 (5): 1271-1289. doi:10.1080/01431161.2015.1011352.

[27]. Shahriari, H., Ranjbar, H. and Honarmand, M. (2013). Image Segmentation for Hydrothermal Alteration Mapping Using PCA and Concentration-Area Fractal Model. Natural Resources Research. 22 (3): 191-206. doi:10.1007/s11053-013-9211-y.

[28]. Hosseinjani Zadeh, M., Tangestani, M.H., Velasco Roldan, F. and Yusta, I. (2014). Sub-pixel mineral mapping of a porphyry copper belt using EO-1 Hyperion data. Advances in Space Research. 53 (3): 440-451. doi:10.1016/j.asr.2013.11.029.

[29]. Hosseinjani, M., Tangestani, M.H., Velasco Roldan, F. and Yusta, I. (2014). Spectral characteristics of alteration zones at porphyry copper deposits; an analysis from Kerman copper belt, SE Iran. Ore Geology Reviews. 62: 191-198. doi:10.1016/j.oregeorev.2014.03.013.

[30]. Waterman, G. and Hamilton, N. (1975). The Sarcheshmeh Porphyry copper deposit. Economic Geology. 70: 568-576.

[31]. Aftabi, A. and Atapour, H. (2010). Alteration Geochemistry of Volcanic Rocks around Sarcheshmeh Porphyry Copper Deposit, Rafsanjan, Kerman, Iran: Implications for Regional Exploration. Resource Geology. 61 (1): 76-90. doi:10.1111/j.1751-3928.2010.00149.x.

[32]. Shafiei, B. and Shahabpour, J. (2012). Geochemical aspects of molybdenum and precious metals distribution in the Sarcheshmeh porphyry copper deposit Iran. Miner Deposita. 47 (5): 535-543. doi:10.1007/s00126-011-0393-0.

[33]. NICICO. (2008). Darrehzar ore reserve estimates. Internal report of National Iranian Copper Industries Company.

[34]. Geological survey of Iran. (1973). Exploration for Ore deposits in Kerman region. Report No, Yu/53. Tehran. Iran: Ministry of Economy Geological Survey of Iran.

[35]. Barzegar, H. (2007). Ph.D. Thesis: Geology, petrology and geochemical characteristics of alteration zones within the Sereidun prospect. Kerman. Iran.

[36]. Salimi, A., Ziaii, M., Hosseinjani Zadeh, M., Amiri, A. and Karimpouli, S. (2015). High performance of the support vector machine in classifying hyperspectral data using a limited dataset. International journal of mining and geoengineering. 36 (5): 253-268.

[37]. Deng, N., Tian, Y. and Zhang, C. (2013). Support Vector Machines: Optimization Based Theory, Algorithms, and Extensions. Published by Chapman and Hall/CRC. 1 edition. 363 P.

[38]. Huang, C., Song, K., Kim, S., Townshend, J.R.G., Davis, P., Masek, J.G. and Goward, S.N. (2008). Use of dark object concept and support vector machines to automate forest cover change analysis. Remote Sensing of Environment. 112 (3): 970-985. doi:10.1016/j.rse.2007.07.023.

[39]. Petropoulos, G.P., Kontoes, C. and Keramitsoglou, I. (2011). Burnt Area Delineation from a uni-temporal perspective based on Landsat TM imagery classification using Support Vector Machines. International Journal of Applied Earth Observation and Geoinformation. 13 (1): 70-80. doi:10.1016/j.jag.2010.06.008.

کاربرد روش کرنل پایه رگرسیون بردار پشتیبان برای طبقه‌بندی زیرپیکسلی مناطق دگرسانی، مطالعه موردی: شناسایی دگرسانی‌های منطقه سرچشمه و نواحی مجاور، کرمان، ایران

امیر سلیمی[1*]، منصور ضیائی[1]، علی امیری[2] و مهدیه حسینجانی‌زاده[3]

۱- دانشکده مهندسی معدن، نفت و ژئوفیزیک، دانشگاه صنعتی شاهرود، ایران

۲- گروه مهندسی کامپیوتر، دانشکده مهندسی، دانشگاه زنجان، ایران

۳- گروه آموزشی زمین‌شناسی، دانشگاه تحصیلات تکمیلی صنعتی و فناوری پیشرفته، ایران

ارسال ۲۰۱۶/۶/۱۹، پذیرش ۲۰۱۶/۱۱/۱۲

* نویسنده مسئول مکاتبات: a.salimi@shahroodut.ac.ir

چکیده:

تصاویر سنجش از دور در دو مقیاس پیکسلی و زیر پیکسلی مطالعه می‌شوند. از دیدگاه طبقه‌بندی تصویر، به مطالعات در مقیاس پیکسل، طبقه‌بندی سخت و در مقیاس زیرپیکسلی، طبقه‌بندی نرم اطلاق می‌شود. نوع سخت بر این فرض استوار است که پیکسل‌های تصویر فقط از یک نوع ماده تشکیل شده و در اصطلاح خالص هستند. در سوی مقابل طبقه‌بندی نرم اشاره به این دارد که پاسخ طیفی هر پیکسل، ترکیبی از پاسخ‌های طیفی اجزا سازنده آن پیکسل است. برای تجزیه طیف‌های ترکیبی به اجزا سازنده، روش‌های تجزیه طیفی مورد استفاده قرار می‌گیرند. روش‌های تجزیه طیفی داده پایه از داده‌های اولیه‌ای به نام نمونه‌های آموزشی برای آموزش الگوریتم استفاده می‌کنند. کارایی این روش‌ها هنگامی که نمونه‌های آموزشی به تعداد کافی در اختیار نباشد تحت تأثیر مشکلات بیش ابعادی قرار گرفته و دقت طبقه‌بندی کاهش می‌یابد. این مشکل اغلب در طبقه‌بندی تصاویر ابرطیفی رخ می‌دهد، چرا که تهیه نمونه‌های آموزشی کافی به طوری که متناسب با تعداد فراوان باندهای تصاویر ابرطیفی باشد، معمولاً مشکل است. در چنین شرایطی استفاده از روش‌های کرنل پایه مثل ماشین بردار پشتیبان (SVM) که در مقابل مشکل بیش ابعادی مقاوم‌تر هستند، می‌تواند مفید واقع شود. در این تحقیق از روش رگرسیون بردار پشتیبان (SVR) برای طبقه‌بندی زیرپیکسلی دگرسانی‌های مناطق سرچشمه، دره زار و سریدون در کرمان استفاده شد. طبقه‌بندی بر اساس ۲۰ نمونه سنگی برداشت شده از مناطق دگرسانی منطقه دره زار انجام شد که ۱۲ نمونه برای آموزش و ۸ نمونه برای اعتبارسنجی نتایج اختصاص یافت. با وجود تعداد نمونه‌های آموزشی کم در مقابل ۱۶۵ باند طیفی قابل استفاده در تصویر هایپریون، دقت مطلوب نتایج به دست آمده نشان داد که SVR برای طبقه‌بندی نرم تصاویر ابرطیفی در شرایط بیش ابعاد می‌تواند انتخاب مناسبی باشد.

کلمات کلیدی: دگرسانی گرمابی، سنجش از دور ابرطیفی، طبقه‌بندی نرم، تجزیه طیفی، رگرسیون بردار پشتیبان.